Electronic Supplementary Information

Exploring the role of ferric source in the structural regulation of ZIF-8 derived nitrogen-doped porous carbon for enhanced photothermal CO_2 cycloaddition

Ying Zhang,[a] Meili Ding,*[a] Yicheng Zhou,[b] Yang Wang,[a] Pan Ma[a] and Jianfeng Yao*[a]

[a]College of Chemical Engineering, Jiangsu Co-Innovation Center of Efficient Processing and Utilization of Forest Resources, Nanjing Forestry University, Nanjing, Jiangsu 210037, China.

[b]School of chemistry and chemical engineering, Jiangsu university of technology, Changzhou, Jiangsu 213001, China

*Corresponding author.

Email: mlding@njfu.edu.cn (MD); jfyao@njfu.edu.cn (JY)

S1. Experimental details

Materials

Zinc nitrate hexahydrate ($Zn(NO_3)_2 \cdot 6H_2O$, 99%) was obtained by Nanjing Chemical Reagent Co., Ltd. Dimethylimidazole (2-MIM, 98%), ferrocene (Fc, 98%), ferric acetylacetonate (FA, 98%), epichlorohydrin (ECH, ≥99.5%), ethyl acetate (99.9%), 1,2-epoxyhexane (99%), styrene oxide (98%), benzyl (R)-(-)-glycidyl ether (99%), epibromohydrin (98%) and tetrabutylammonium bromide (TBAB, analytical reagent (AR)) were purchased from Aladdin. Ferric citrate (FC, AR) was provided by Macklin Reagent Co., Ltd. Epoxypropyl phenyl ether (99%) was obtained from energy chemical. Methanol (MeOH, AR) and ethanol (AR) were obtained by Sinopharm Chemical Reagent Co., Ltd. All chemicals are obtained commercially and used without further treatment. The CO_2 gas was supplied from a gas cylinder (99.8% purity).

Synthesis of ZIF-8

ZIF-8 was prepared based on a previously reported protocol with slight modifications.[S1] $Zn(NO_3)_2 \cdot 6H_2O$ (11.90 g, 40 mmol) was dissolved in 400 mL of MeOH to obtain a transparent solution. Upon adding 2-MIM (26.27 g, 320 mmol), the mixture was then magnetically stirred at 600 rpm for 1 h, followed by aging at room temperature (RT) for 24 h. The white precipitates were washed with MeOH three times, and then dried at 80 ℃ for 12 h to yield white solid.

Synthesis of Fe functionalized NPCs

1.00 g of ZIF-8 powder was immersed in 20 mL MeOH solution containing Fc (42.60 mg, 0.229 mmol). After stirring at RT for 24 h, MeOH was removed by rotary evaporation at 60 ℃ for 1 h. The resulting solid was then calcined for 2 h at 900 ℃ under argon atmosphere with a heating rate of 5 ℃/min to give Fc-NPC. FA-NPC and FC-NPC were synthesized according to the same method of Fc-NPC, except for replacing Fc with the same molar amounts of FA and FC.

Catalytic performance evaluation

Typically, catalyst (30 mg) was suspended in ECH (234 μL, 2.98 mmol) with TBAB (12 mg, 0.0372 mmol) and placed in a 5 mL flask. After discharging the air by purging with CO_2, the flask was connected by a CO_2 balloon. The reaction was performed under the irradiation of a 300 W Xenon lamp with an illumination intensity of 400 mW/cm^2. The catalytic yields and selectivities were analyzed using gas chromatography (GC) at the end of reactions. To test the recyclability of Fc-NPC, the catalyst was separated from the reaction system by centrifugation, washed with ethanol several times, and carefully dried at 80 ℃ under vacuum for using in the next reaction. The coupling of CO_2 and other epoxides over Fc-NPC was conducted by a similar procedure to ECH, except that the light intensity was increased to 500 mW/cm^2.

S2. Material characterizations

The crystal structure of samples was studied by means of X-ray diffraction (XRD) analysis using Rigaku Ultima IV diffractometer. The specific surface area, pore size

distribution and CO_2 sorption isotherm of samples were measured on a Micromeritics TriStar II instrument. Scanning electron microscopy (SEM) and energy dispersive X-ray spectrometry (EDS) analysis were performed on Regulus 8100 to characterize the morphologies and elemental distribution of samples. The transmission electron microscopy (TEM) and high-resolution TEM (HRTEM) images were acquired on FEI-Tecnai G2 F30. The surface chemistry analysis of NPCs was conducted through X-ray photoelectron spectroscopy (XPS, AXIS UltraDLD). Solid-state UV-vis diffuse reflectance spectra were recorded on a Shimadzu UV-2600 spectrophotometer. The catalytic yield and selectivity were determined by using a GC (HF-901A, Shandong Hui fen Instrument Co., Ltd., China). The surface temperature of samples was were monitored by a thermal imaging camera (HF-901). The contents of Fe and Zn elements in sample were measured by inductively coupled plasma-optical emission spectrometry (ICP-OES, Thermo Fisher iCAP PRO). The elemental analysis of C, N, and H was performed using 2400 II (Perkin Elmer, USA)

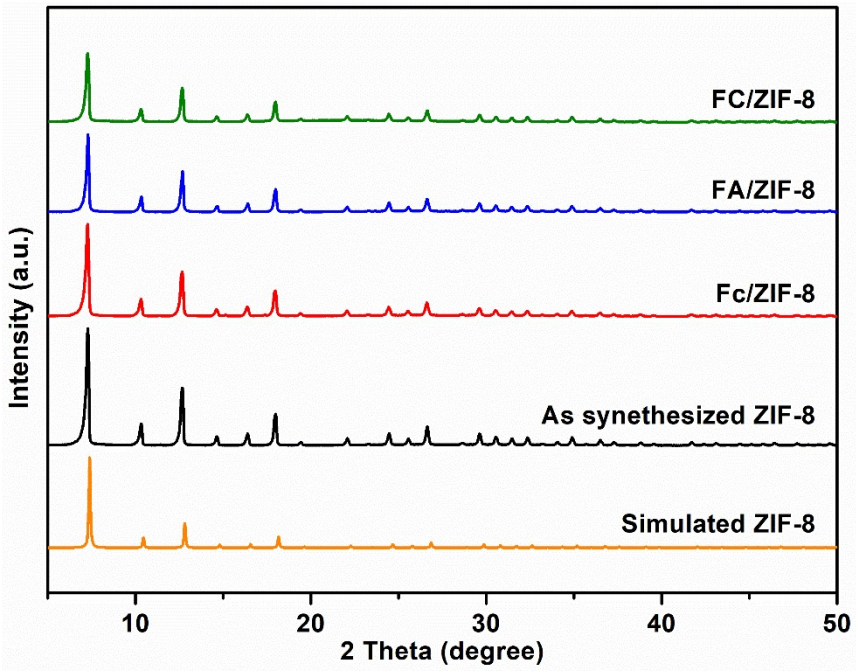

Fig. S1 XRD patterns of simulated ZIF-8, as synthesized ZIF-8, Fc/ZIF-8, FA/ZIF-8, and FC/ZIF-8.

Fig. S2 Digital photographs of ZIF-8, Fc/ZIF-8, FA/ZIF-8, and FC/ZIF-8.

Table S1 The content of Fe and Zn elements obtained from the ICP and elemental analysis results of three NPC samples.

Sample	Fc-NPC	FA-NPC	FC-NPC
Fe (at. %)	0.51	3.92	2.60
Zn (at. %)	1.95	-	-
C (at. %)	70.02	78.02	80.38
H (at. %)	1.78	0.09	0.11
N (at. %)	3.59	2.31	2.63

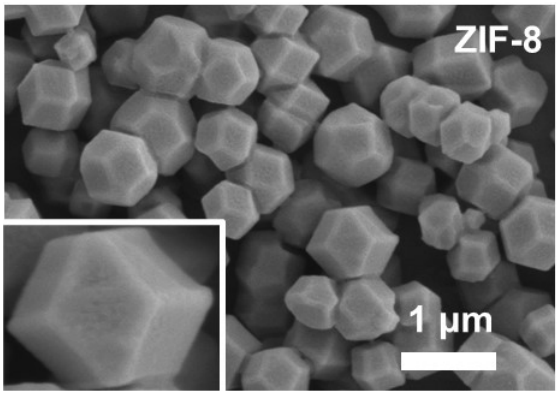

Fig. S3 SEM image of ZIF-8. Inset: local enlarged view.

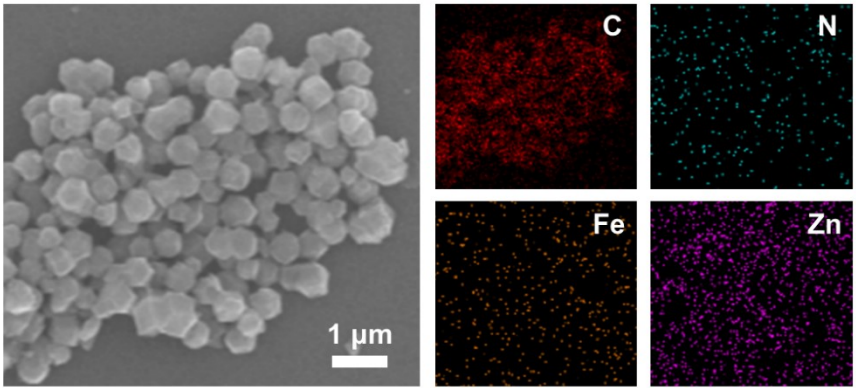

Fig. S4 Elemental maps of Fc-NPC revealed by EDS analysis.

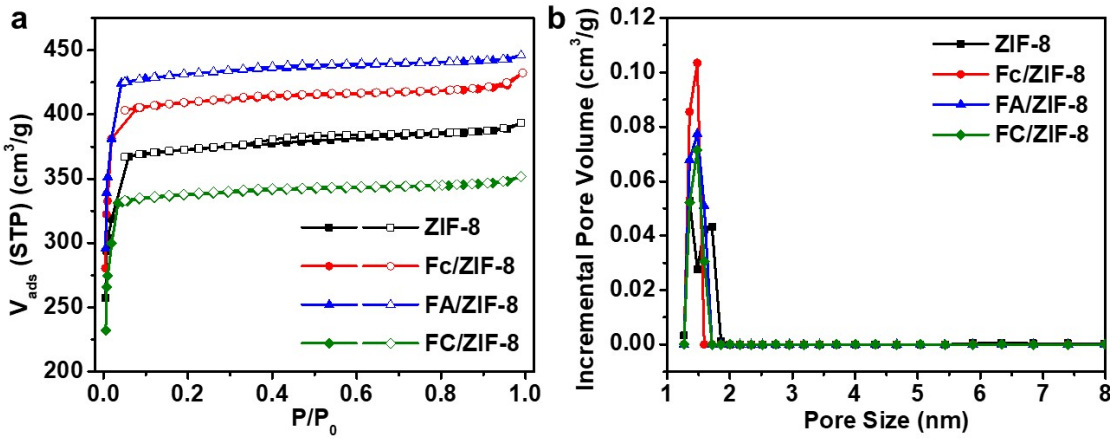

Fig. S5 (a) Nitrogen (N_2) sorption isotherms and (b) pore size distribution curves of ZIF-8, Fc/ZIF-8, FA/ZIF-8, and FC/ZIF-8.

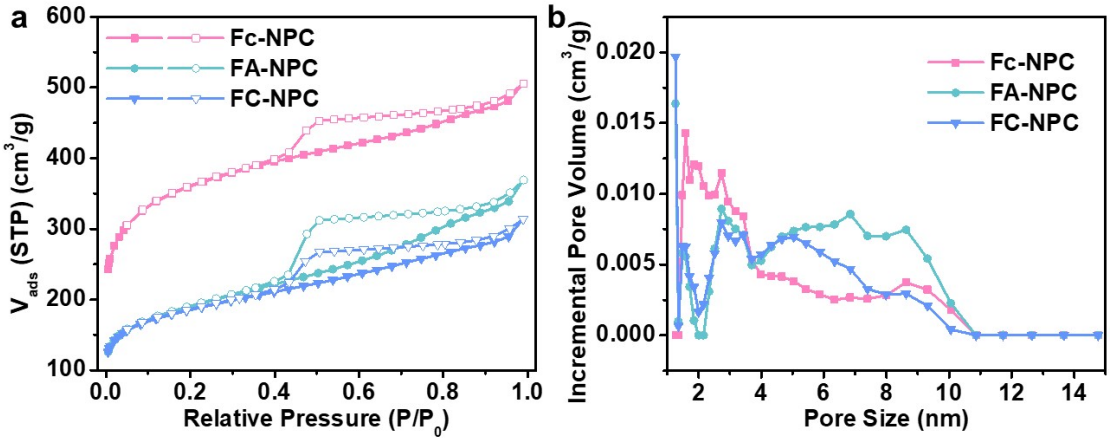

Fig. S6 (a) N_2 sorption isotherms and (b) pore size distribution curves of Fc-NPC, FA-NPC, and FC-NPC.

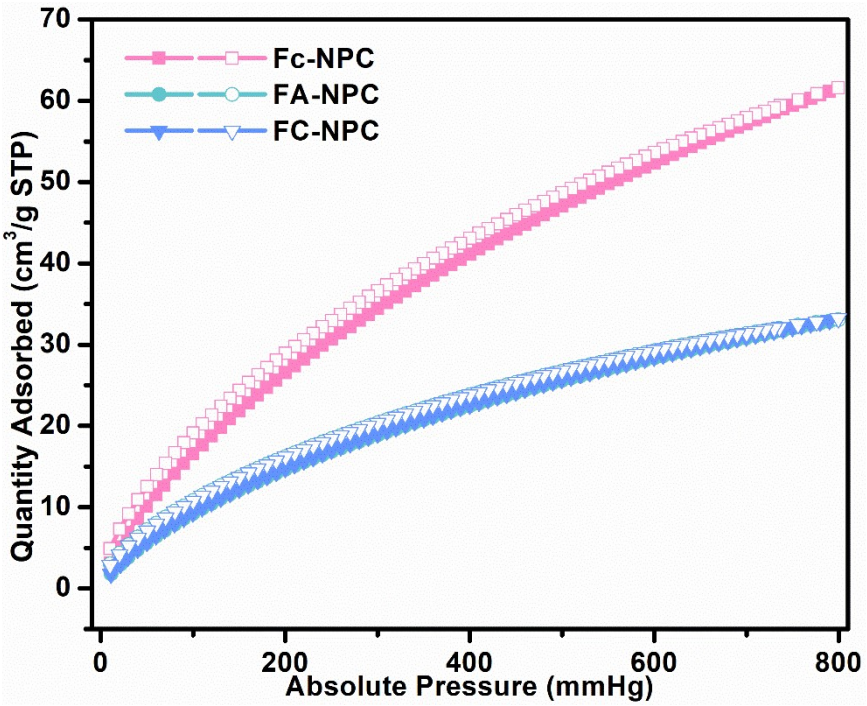

Fig. S7 CO_2 sorption isotherms of Fc-NPC, FA-NPC, and FC-NPC at 273 K.

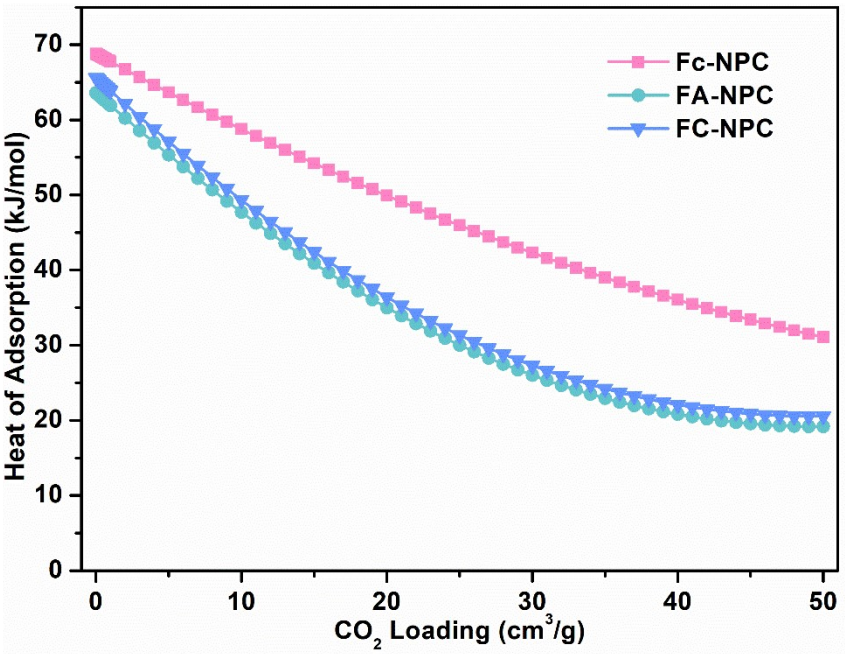

Fig. S8 Isosteric heat of CO_2 adsorption for Fc-NPC, FA-NPC, and FC-NPC.

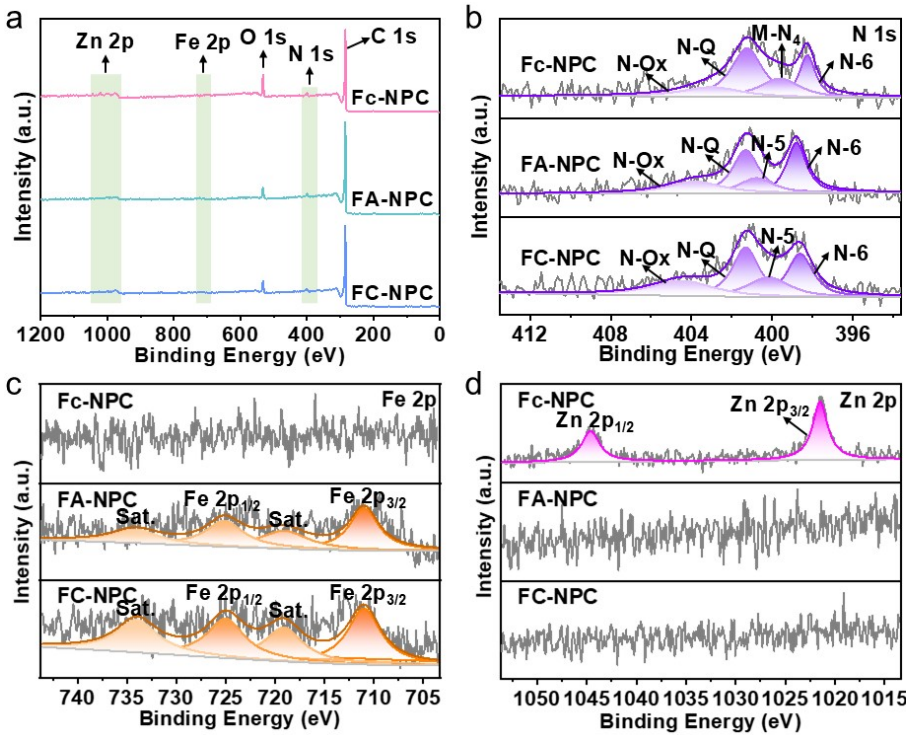

Fig. 9 (a) XPS wide-scan spectra and (b-d) high-resolution XPS spectra of N 1s, Fe 2p, and Zn 2p of Fc-NPC, FA-NPC, and FC-NPC.

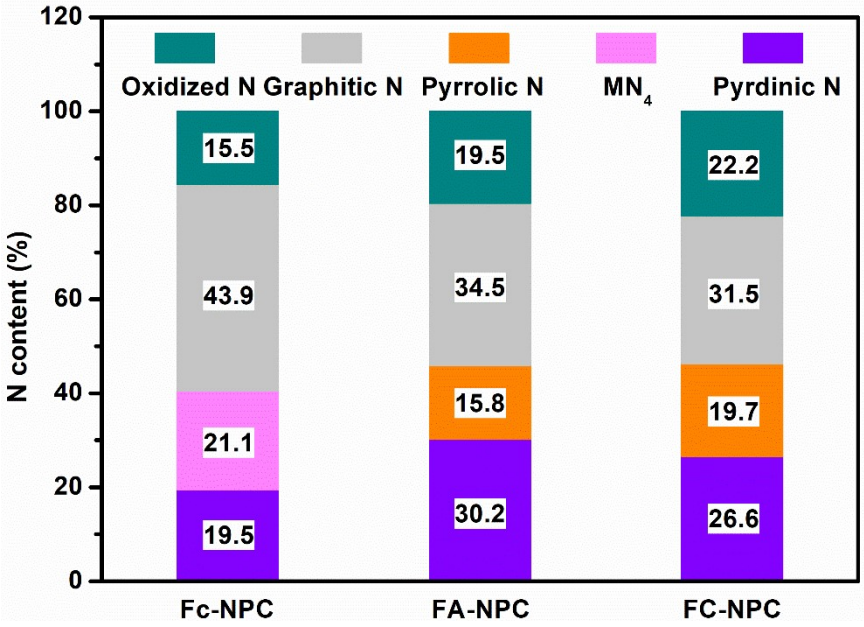

Fig. S10 The relative content of different N species in three NPC samples determined by XPS analysis.

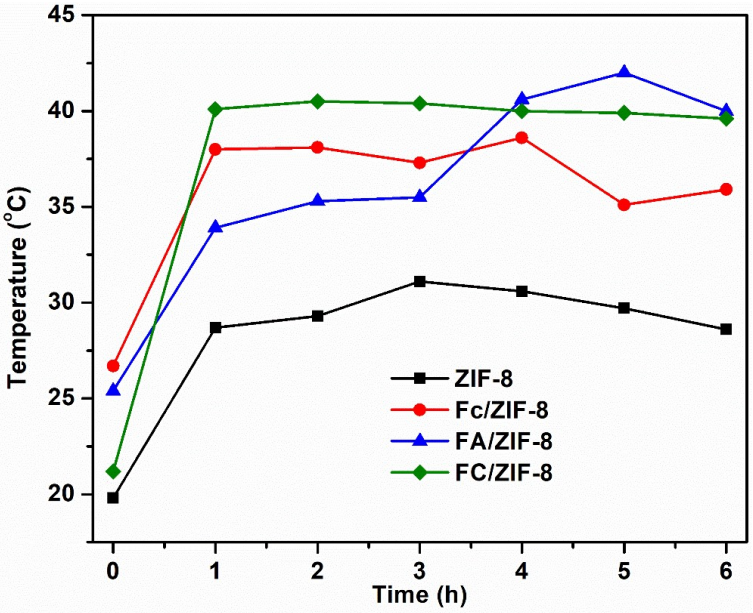

Fig. S11 Temperature changes of reaction systems in the presence of ZIF-8, Fc/ZIF-8, FA/ZIF-8, or FC/ZIF-8 under light irradiation.

Table S2 A summary of our catalyst and the reported catalysts for photodriven CO_2 cycloaddition.

Catalyst	Epoxide	Co-catalyst	Solvent	CO_2 pressure (bar)/light intensity (mW/cm^2)/t (h)	Yield (%)	Ref.
Fc-NPC		TBAB	/	1/500/6	100	This work
Br-CN-1-550		/	DMF	1/300/10	90	[S2]
NB-BC		TBAB	/	1/400/6	99	[S3]
ZNPC-600		TBAB	MeCN	1/300/6	99	[S4]
ZnO/NCO-L		TBAB	MeCN	1/120/6	76	[S5]
BHNC-(0.025, 800)	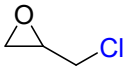	TBAB	DMF	1/300/8	97	[S6]
TbN_4B_2/C		TBAB	/	1/400/6	92	[S7]
ZNC-800		TBAB	/	1/1000/10	88	[S8]
ZnS/NPC-2		TBAB	DMF	1/152.5/12	98	[S9]
Al–N–C		TBAB	DMF	1/400/16	90	[S10]
HPC-800		TBAB	DMF	1/300/10	96	[S11]
CTS-800		TBAB	/	1/350/10	68	[S12]

Fc-NPC		TBAB	/	1/500/8	95	This work
Al–N–C		TBAB	DMF	1/400/12	95	[S10]
HPC-800		TBAB	DMF	1/300/10	94	[S11]
Zn-N-HOPCPs	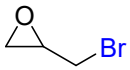	TBAB	/	1/300/10	92	[S13]
Zn SA-NC		TBAB	DMF	1/300/16	99	[S14]
Ni-BNCNTs@HMPs-NH_2		/	/	1/400/12	99	[S15]
Fc-NPC		TBAB	/	1/500/24	88	This work
BHNC-(0.025, 800)		TBAB	DMF	1/300/36	91	[S6]
ZNC-800	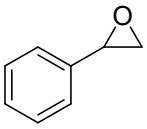	TBAB	/	1/1000/20	84	[S8]
HPC-800		TBAB	DMF	1/300/48	67	[S11]
Zn-N-HOPCPs		TBAB	/	1/300/48	68	[S13]

Ni-BNCNTs@HMPs-NH_2		/	/	1/400/48	92	[S15]
13.3 Ti-CNO		TBAB	/	1/300/6	98	[S16]
Fc-NPC		TBAB	/	1/500/16	100	This work
NB-BC		TBAB	/	1/500/24	100	[S3]
Zn-N-HOPCPs	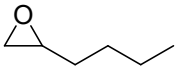	TBAB	/	1/300/36	88	[S13]
Ni-BNCNTs@HMPs-NH_2		/	/	1/400/36	94	[S15]
Fc-NPC		TBAB	/	1/500/18	100	This work
ZnS/NPC-2		TBAB	DMF	1/152.5/12	88	[S9]
Zn-N-HOPCPs	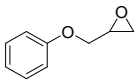	TBAB	/	1/300/24	91	[S13]
Ni-BNCNTs@HMPs-NH_2		/	/	1/400/24	96	[S15]
Fc-NPC	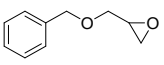	TBAB	/	1/500/24	100	This work

NB-BC	TBAB	/	1/500/24	100	[S3]
BHNC-(0.025, 800)	/	/	1/400/24	96	[S6]
HPC-800	TBAB	DMF	1/300/24	92	[S11]

S3. Reaction mechanism

As shown in Fig. S12, Zn and Fe atoms can serve as Lewis acid sites to coordinate with the oxygen atoms of epoxides, promoting the polarization of the β–C–O bond of substrates. At the same time, CO_2 molecules were adsorbed and activated by pyridine N sites within Fc-NPC. Afterwords, the nucleophilic attack of Br^- ions from TBAB on the less sterically hindered carbon atom of epoxide produced a ring-opened intermediate. Sequentially, this intermediate can act as a nucleophilic reagent to attack activated CO_2, thereby affording an alkyl carbonate compound. Ultimately, cyclic carbonate was obtained through an intramolecular ring-closure, freeing Br^- ions and Fc-NPC.

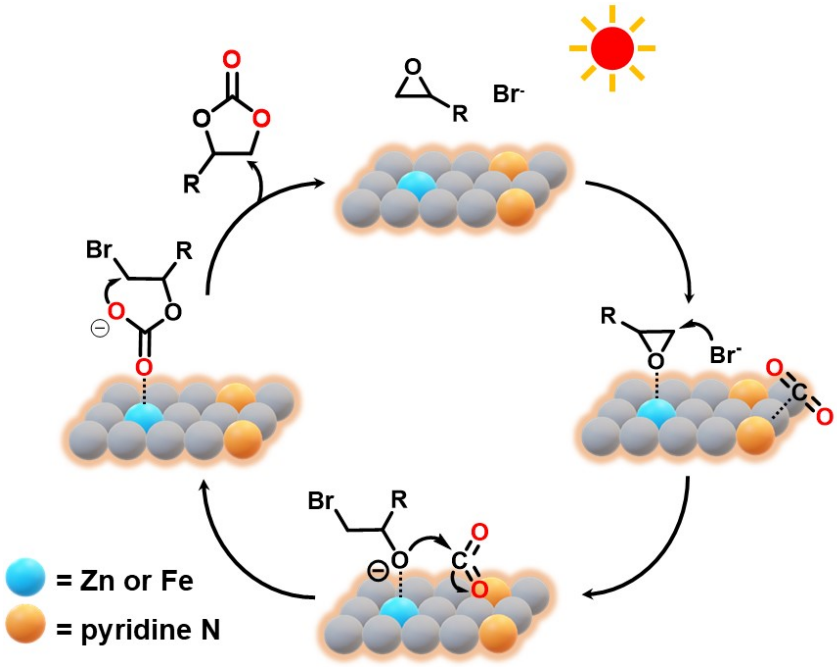

Fig. S12 Proposed reaction mechanism for Fc-NPC-catalyzed CO_2 cycloaddition with epoxides with the aid of TBAB.

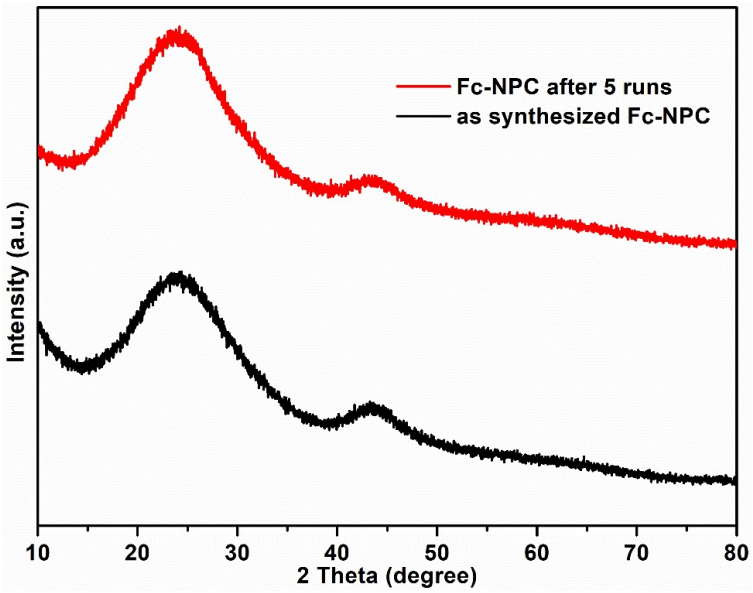

Fig. S13 XRD patterns of Fc-NPC before and after 5 runs of photothermally catalytic CO_2 cycloaddition.

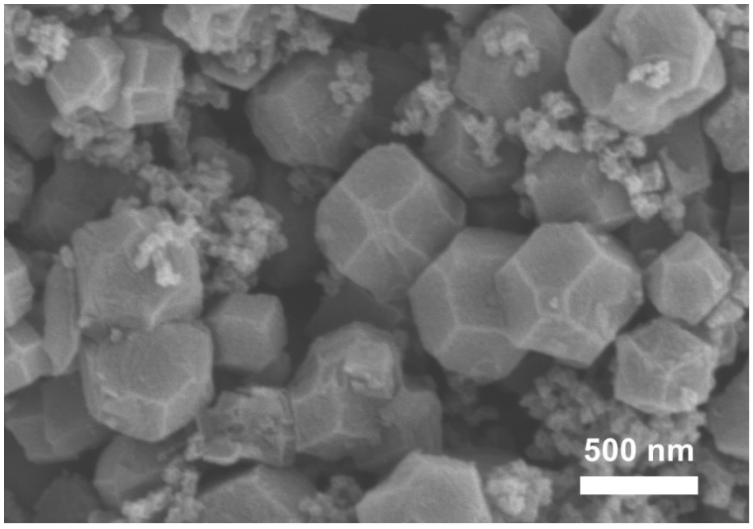

Fig. S14 SEM image of Fc-NPC after 5 runs of photothermally catalytic CO_2 cycloaddition.

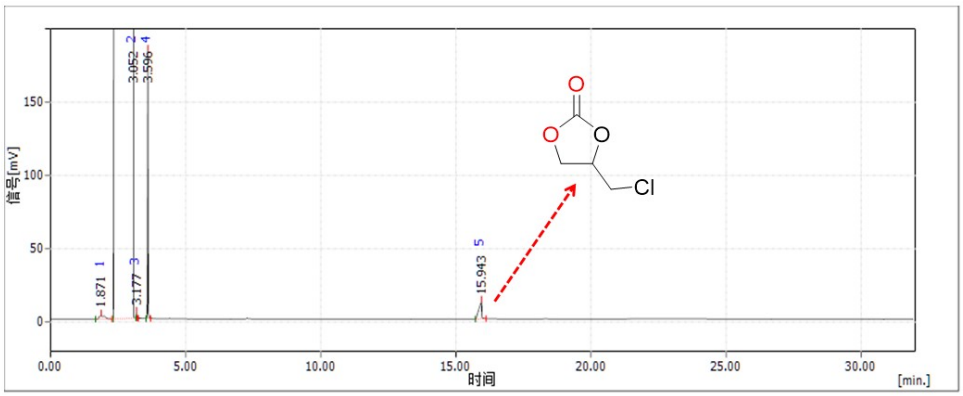

Fig. S15 Gas chromatogram of CO_2 cycloaddition with ECH catalyzed by Fc-NPC.

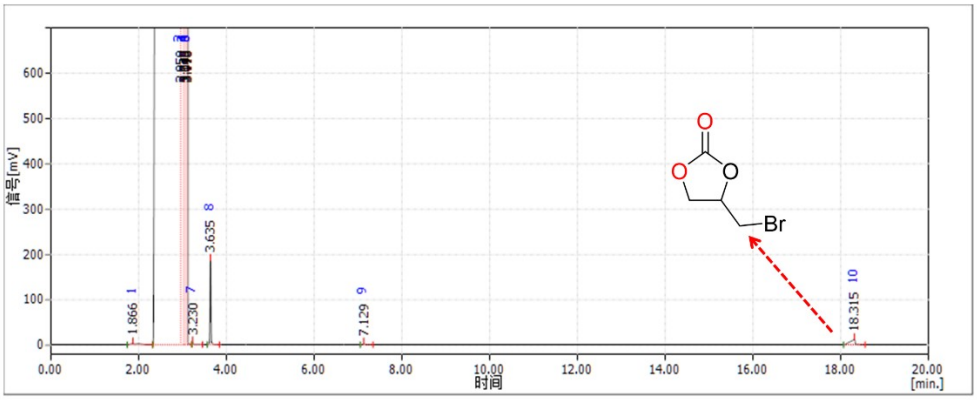

Fig. S16 Gas chromatogram of CO_2 cycloaddition with epibromohydrin catalyzed by Fc-NPC.

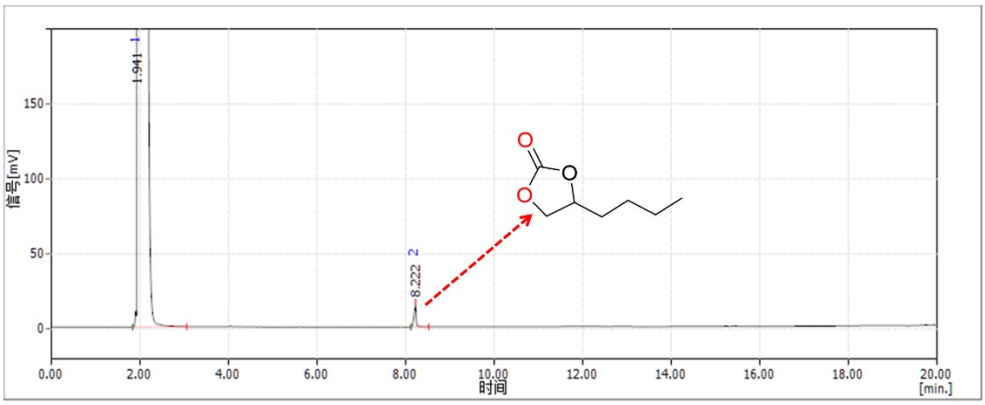

Fig. S17 Gas chromatogram of CO_2 cycloaddition with 1,2-epoxyhexane catalyzed by Fc-NPC.

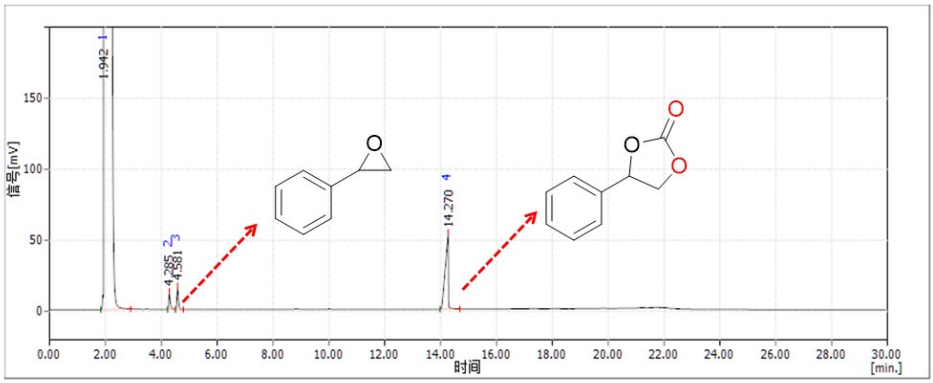

Fig. S18 Gas chromatogram of CO_2 cycloaddition with styrene oxide catalyzed by Fc-NPC.

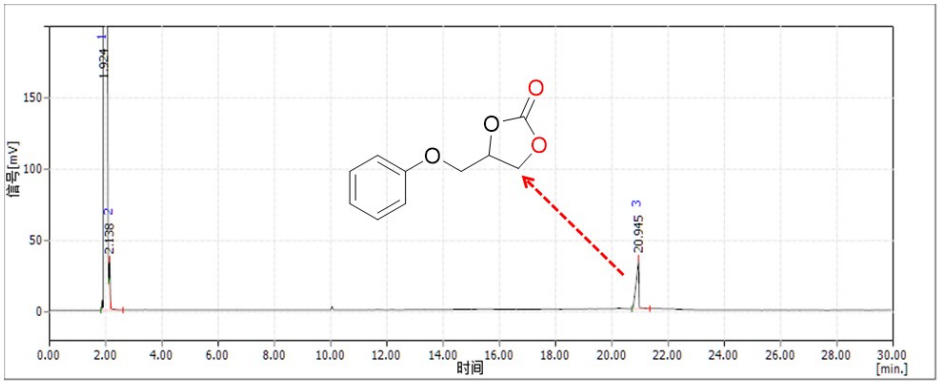

Fig. S19 Gas chromatogram of CO_2 cycloaddition with epoxypropyl phenyl ether catalyzed by Fc-NPC.

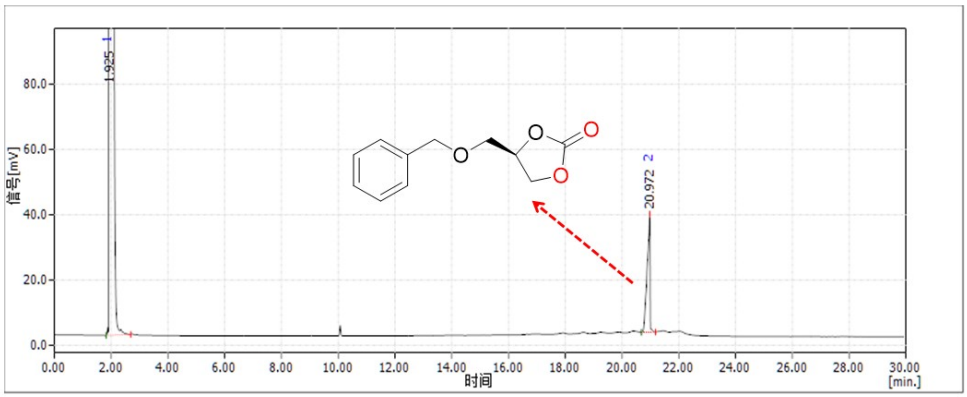

Fig. S20 Gas chromatogram of CO_2 cycloaddition with benzyl (R)-(-)-glycidyl ether catalyzed by Fc-NPC.

References

S1. Y. Ye, F. Cai, H. Li, H. Wu, G. Wang, Y. Li, S. Miao, S. Xie, R. Si, J. Wang and X. Bao, *Nano Energy*, 2017, **38**, 281-289.

S2. T. Wang, F. Chen, L. Jiang, J. Li, K. Chen and J. Gao, *Inorg. Chem.*, 2024, **63**, 4224-4232.

S3. W. Rong, M. Ding, Y. Wang, S. Kong and J. Yao, *Sep. Purif. Technol.*, 2025, **353**, 128427.

S4. W. Rong, M. Ding, P. Ma, S. Kong and J. Yao, *J. Ind. Eng. Chem.*, 2024, **129**, 682-690.

S5. C. Duan, M. Ding, Y. Feng, M. Cao and J. Yao, *Sep. Purif. Technol.*, 2022, **285**, 120359.

S6. T. Wang, F. Chen, H. An, K. Chen and J. Gao, *J. Solid State Chem.*, 2024, **332**, 124570.

S7. Y. Xu, P. Wang, X. Zhan, W. Dai, Q. Li, J. Zou and X. Luo, *J. Colloid Interf. Sci.*, 2024, **673**, 134-142.

S8. Y. Liu, Y. Chen, Y. Liu, Z. Chen, H. Yang, Z. Yue, Q. Fang, Y. Zhi and S. Shan, *J. Catal.*, 2022, **407**, 65-76.

S9. F. Tang, L. Wang, L. Ma, Y. Fang, J. Huang and Y.-N. Liu, *J. CO_2 Util.*, 2021, **45**, 101431.

S10. Q. Yang, H. Peng, Q. Zhang, X. Qian, X. Chen, X. Tang, S. Dai, J. Zhao, K. Jiang, Q. Yang, J. Sun, L. Zhang, N. Zhang, H. Gao, Z. Lu and L. Chen, *Adv. Mater.*, 2021, **33**, 2103186-2103194.

S11. Q. Yang, C. C. Yang, C. H. Lin and H. L. Jiang, *Angew. Chem. Int. Ed.*, 2019, **58**, 3511-3515.

S12. Z. Yang, Y. Xie, Y. Feng and J. Yao, *J. Environ. Chem. Eng.*, 2024, **12**, 112310.

S13. Y. Guo, L. Feng, C. Wu, X. Wang and X. Zhang, *J. Catal.*, 2020, **390**, 213-223.

S14. L. Gong, J. Sun, Y. Liu and G. Yang, *J. Mater. Chem. A*, 2021, **9**, 21689-21694.

S15. Y. Guo, W. Chen, L. Feng, Y. Fan, J. Liang, X. Wang and X. Zhang, *J.Mater. Chem. A*, 2022, **10**, 12418-12428.

S16. Y. Wang, H. Liu, Q. Shi, Z. Miao, H. Duan, Y. Wang, H. Rong and J. Zhang, *Angew. Chem. Int. Ed.*, 2024, **63**, e202404911.